

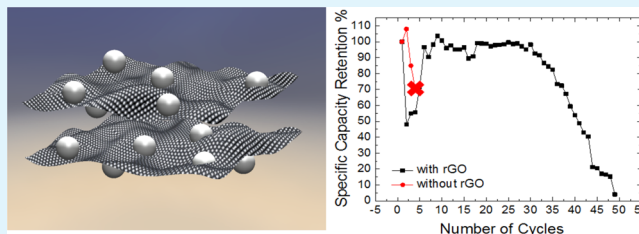
# Improving Performance and Cyclability of Zinc–Silver Oxide Batteries by Using Graphene as a Two Dimensional Conductive Additive

Dilek Ozgit, Pritesh Hiralal,\* and Gehan A.J. Amaratunga

Electrical Engineering Division, Department of Engineering, University of Cambridge, 9 JJ Thomson Avenue, Cambridge CB3 0FA, United Kingdom

## S Supporting Information

**ABSTRACT:** In this article, the use of reduced graphene oxide (rGO) as a high-surface-area conductive additive for enhancing zinc–silver oxide (Zn–Ag<sub>2</sub>O) batteries is reported for the first time. Specific capacity, rate capability and cyclability are all improved with the addition of 5% thermally reduced graphene oxide to the electrode. It is shown that the rGO morphology becomes more beneficial as the active materials tend toward the nanoscale. The combination results in a better utilization of the active material, which in turn improves the specific capacity of the zinc–silver oxide batteries by ca. 50%, as a result of the more intimate contact with the nano (~50 nm) electrode particles. The resulting rGO network also creates a high-surface-area conducting template for ZnO electrodeposition upon discharge, significantly reducing the overall particle size of the ZnO deposit, thus inhibiting the formation of dendrites, and increasing the number of achievable cycles from 4 to >160 with a basic cellulose separator. The morphology of the electrodes and its electrochemical parameters are studied as a function of cycling.



**KEYWORDS:** zinc, silver, secondary batteries, reduced graphene oxide, dendrites

## 1. INTRODUCTION

Zinc is widely used as anode material in primary and secondary batteries such as Zn–MnO<sub>2</sub> (Leclanché cells),<sup>1–3</sup> Zn–Ag<sub>2</sub>O,<sup>4,5</sup> Ni–Zn,<sup>6</sup> and Zn–air.<sup>7,8</sup> because of relatively high electrode potential and low weight, reversibility, low overpotential, high rate discharge ability, compatibility with aqueous electrolyte, and low cost.<sup>9–11</sup> In particular, zinc/silver oxide batteries have been used in some consumer electronic devices such as watches, film cameras, hearing aids, toys, glucose monitors, and calculators as well as in more demanding military applications because of their high energy and high power densities. They have one of the highest power densities among commercial rechargeable batteries up to 600 W kg<sup>-1</sup> continuous or 2500 W kg<sup>-1</sup> for pulsed power.<sup>5</sup> High specific energy of 300 W h kg<sup>-1</sup> (vs ~150 Wh kg<sup>-1</sup> for Li-ion batteries)<sup>12</sup> low self-discharge rate of ~5% per month, and a flat voltage discharge curve also make zinc silver batteries attractive.<sup>5</sup> They are inherently safe (because they are aqueous based) and environmentally friendly,<sup>13</sup> albeit the high cost of silver. Even that may be circumvented via recycling schemes that have been proposed.<sup>14</sup>

However, zinc electrodes also suffer from various inherent problems. One of these challenges is associated with the shape change of zinc anode originating from its high solubility in alkaline electrolytes and rapid electrochemical kinetics.<sup>9,15</sup> Zinc oxide formed during discharge is dissolved in the electrolyte up to a certain extent and redeposited in the form of needle-like dendrites in different regions.<sup>5,9,10</sup> This results in active material

lost, penetration of the dendrites through the separator causing short circuit, and the loss of ideal electrode morphology after the first cycle. Many different approaches have been studied to reduce the shape change of the zinc anode.<sup>16</sup> Recently, it was shown that the presence of finer zinc particles with less energetic facets that are less soluble improves the performance of the zinc electrode.<sup>17</sup> It has been suggested that using a higher amount of zinc than that required for stoichiometric equilibrium compensates zinc losses to the solution during charge and discharge.<sup>10,15</sup> Much work has been done on addition of corrosion and shape inhibitors at electrodes or electrolyte that have a hydrogen overvoltage higher than that of zinc. Binders such as PTFE, potassium titanate, or other polymers that provide mechanical support have been only partially successful.<sup>10,18</sup> Apart from the electrode material, developments in the separator have played a key role in increasing cycle life in zinc/silver oxide batteries. The use of multilayer separators, a positive interseparator made of nylon or polypropylene, a negative interseparator made of asbestos and potassium titanate, and an ion exchange separator such as cellophane have been adopted and proven effective in preventing zinc dendrite penetration, as well as silver migration. However, the multilayer separator poses some limitations; it results in an increased cost, complexity, and a

Received: July 25, 2014

Accepted: November 4, 2014

Published: November 24, 2014

higher internal resistance.<sup>10</sup> A number of new battery designs have been demonstrated recently, including printed<sup>19,20</sup> and

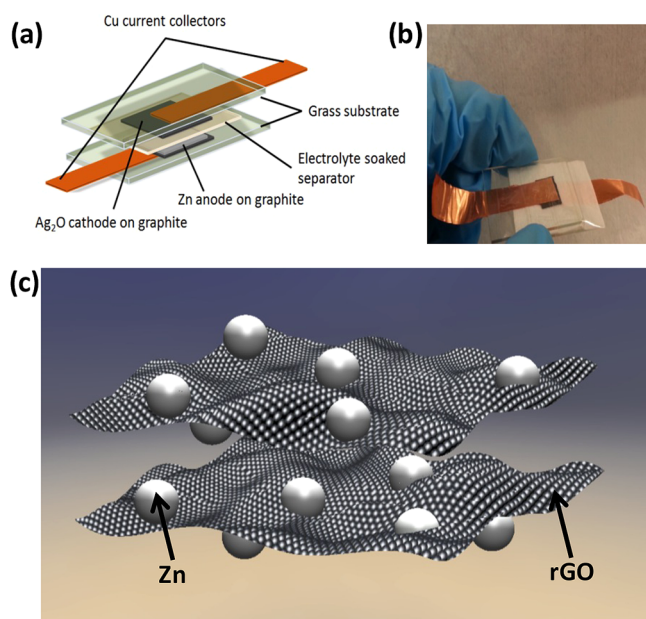


**Figure 1.** (a) Diagrammatic structure of the batteries fabricated in this work. (b) Photograph of a typical device. (c) Schematic showing the structure of the proposed electrode, with the Zn nanoparticles embedded within a conducting rGO matrix.

stretchable versions using silver nanowires;<sup>21</sup> however, the same fundamental difficulties remain.

In any case, an additive forming a network of electrochemically stable, conducting paths is important for reducing the internal resistance of the electrodes, as in this system, one of the electrodes is always in the oxide (poorly conducting) state. Optimisation of the morphology of the conductive network can lead to an overall improvement in the performance of the battery. In this work, we introduce 2D reduced graphene oxide (rGO) as a high-surface-area conductive and structural additive to the electrodes in the zinc/silver battery. rGO is a low cost alternative to graphene, produced in bulk from chemically exfoliated graphite. The benefits of rGO additives in battery electrodes have been recently demonstrated in lithium-ion battery (LIB) electrodes.<sup>22–25</sup>

The use of nanostructured active materials in battery electrodes has permitted higher energy and power densities as a result of the better utilization of the active material and a reduction in ion and electron diffusion lengths, providing a large surface area for electrode–electrolyte interaction.<sup>26,27</sup> For this particular case of a nanoparticle based electrode, a 2D high surface area conductive additive such as rGO is effective in maximizing the number of particles which are in direct electrical contact with the conductive carbon matrix. Synergistically, the nanoparticles prevent the restacking of rGO.

The results show the rGO matrix brings significant advantages to the battery performance: (i) it provides a high surface area, continuous 3-D conducting network, even after many

### Zn – Electrode Morphology

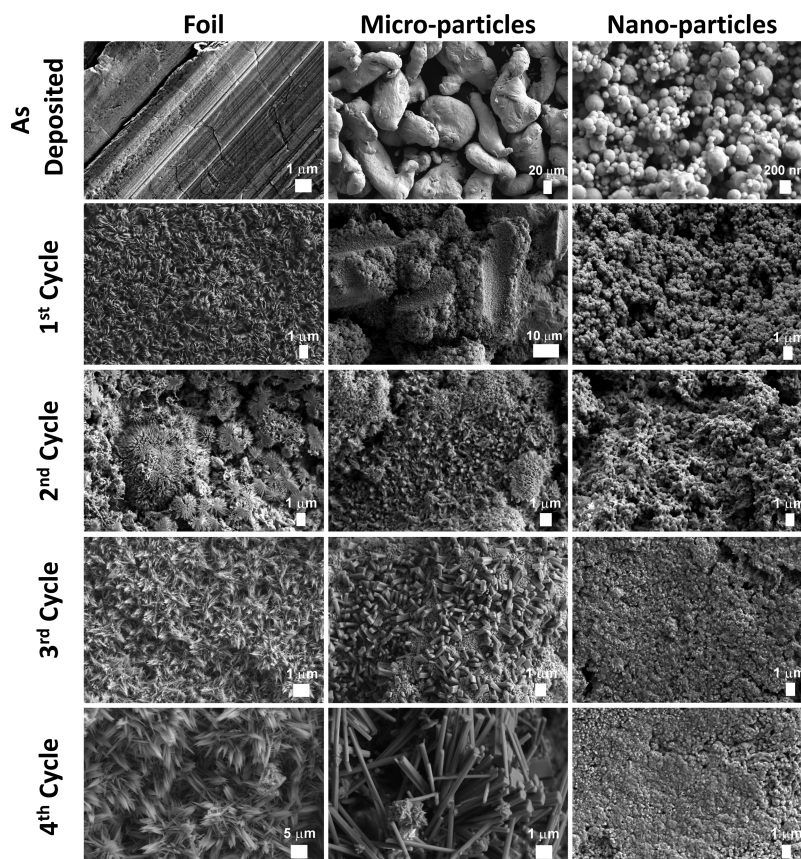


**Figure 2.** SEM images of the development of Zn electrode structure as a function of discharge cycle. The development is studied for 3 different Zn electrode morphologies (foil, microgranules, and nanoparticles).



cycles of charge and discharge,<sup>22–25</sup> (ii) mitigates volume expansion and shape change of nanostructured active material because of its flexible nature.<sup>22</sup> (iii) provides a large surface area on which it is favorable for ZnO to regrow upon discharging, reducing the overall size of the ZnO nanowires or dendrites which result in the device shorting as well as reducing agglomeration of the nanostructured electrode. This results in an increase in cyclability from 4 to >160 cycles with a basic cellulose separator and no further additives.

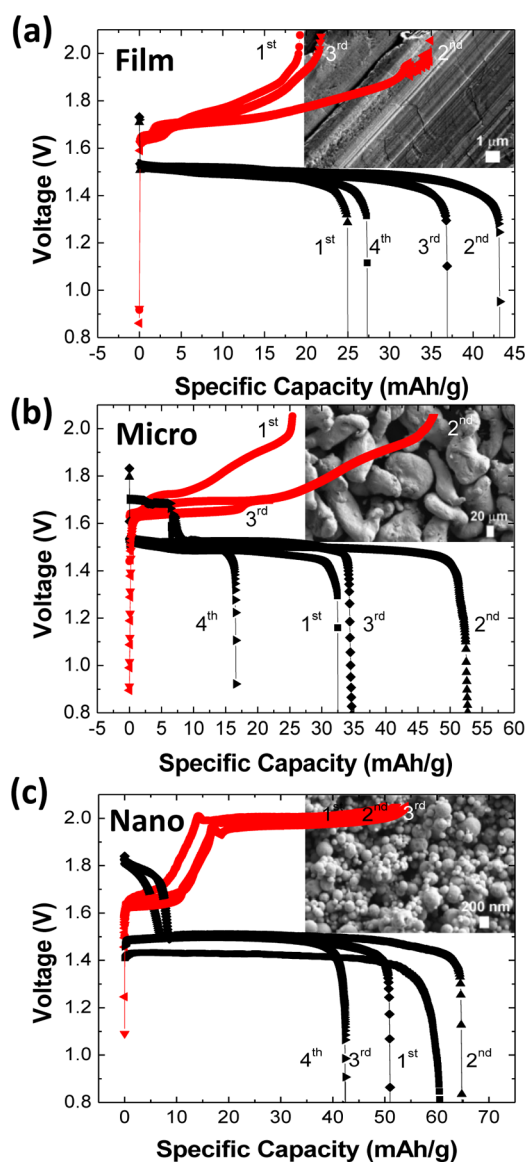
## RESULTS AND DISCUSSION

Figure 1 shows the structure of the batteries fabricated. Batteries consisted of 1 cm<sup>2</sup> electrodes, with the active material pasted onto a graphite plate. The active material (Zn and Ag<sub>2</sub>O) was blended with rGO. Glass slides were used as a structural material for convenience but serve no other function.

It is well-known that particle size has a significant effect both on the distance and speed of ion diffusion,<sup>28,29</sup> to the point where certain electrodes (e.g., LiFePO<sub>4</sub> for Li-ion batteries) are only made possible using nanosized particles. Large particles and low surface areas pose limitations for high power batteries. In general, given the charging/discharging of batteries is a bulk process (i.e., it uses the bulk of the electrode), having a larger surface area generally results in a better utilization of the electrode due to shorter solid state diffusion distances. This is the case for Zn/Ag batteries. Three forms of Zn were studied to understand the effect, namely foil, microgranules (~100 μm) and nanoparticles (~50 nm). Surface area information for these particles is available in the Supporting Information. Figure 2 shows the development of the electrode morphology as a function of cycle number for these electrodes. ZnO, a product of Zn/Ag battery discharge, has a wurtzite structure, and tends to grow as elongated structures in the (0 0 1) direction. This habit is observed in the bulk battery electrodes and the rods become more pronounced with each cycle, reaching >10 μm. The nanoparticle electrode, however, does not show this behavior, but instead the particles tend to agglomerate with time. It has been shown that as the particle size of zinc increases, the byproduct ZnO particle size increases too and the product dissolves with a higher rate and up to a larger extent in the KOH solution of same concentration.<sup>17</sup> The increased resistance to solvation of the zinc oxide nanoparticles in the electrolyte results in a more stable zinc electrode with less shape change.

The capacity, cyclability, and electrode morphology of several morphologies of zinc was studied. Without the use of a multilayer separator, it was only possible to cycle all these cells only 4 times. The capacity of the cells increased with Zn surface area, that is,  $C_{\text{foil}} < C_{\text{microgranules}} < C_{\text{nanoparticles}}$ . Cycling data is shown in Figure 3. All cycling was done at 5 mA charge and discharge current. Devices were discharged to 0.8 V and charged to 2.05 V. The surface area of the electrode also correlates with the capacity of the first conditioning cycle. With the foil electrode, the first cycle shows a lower capacity than subsequent cycles, whereas in the micro and nano case, as surface area increases, the second cycle shows the highest capacity.

However, cyclability was still poor in all cases. The addition of rGO to the electrode paste had a significant effect in aiding this. It was noted the contribution of rGO becomes more significant when the active material is used in the form of nanopowder, which we ascribe to the larger area of contact. The GO product resulting from the modified Hummers' method results in a wide size distribution of sheet widths, ranging from 20 nm to 2 μm as confirmed by SEM. The GO flakes are mostly single



**Figure 3.** Cycling performance of devices made from Zn (a) foil, (b) microgranules, and (c) nanoparticles. An increase in capacity with surface area is observed from ~43–65 mAh/g. Discharge current: 5 mA (~42 mA/g).

to few layers with about 1 nm thickness as measured by AFM. However, upon the production of rGO some inevitable restacking occurs. The amount of rGO on the electrode was optimized to be 40:2 (Zn nanopowder/rGO) by weight (see the Supporting Information), and showed several significant benefits, including lower internal resistance of the device, higher utilization of the electrode and a significant reduction in the size of the dendrites (10 μm to <2 μm). These effects are summarized in Figure 4.

Electrochemical impedance spectroscopy (EIS) shows, as expected, reduced device resistance upon the addition of rGO, as a result of having a conducting network available in the oxidized state of the electrode. Cyclic voltammetry was also conducted. The addition of rGO leads to an increase in the size of the oxidation and reduction peaks, suggesting a better utilization of the electrode material. The shift toward positive potential of the main discharge peak during reverse sweep suggests a faster rate of reaction on the rGO electrodes, once again, less limited by the poor conductivity of the oxide states.

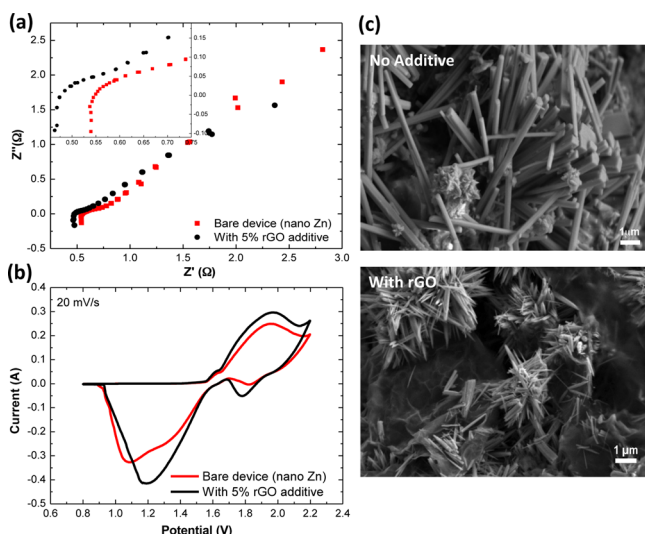


**Figure 4.** (a) Impedance spectra (0.01 to 100 000 Hz) comparing cells with Zn electrodes with and without rGO (b) Cyclic voltammogram of comparing the same two devices (c) SEM images showing the effect of rGO on cycling electrodes made with Zn microgranules. rGO strongly affects the size of the resulting dendrites.

However, as well as being a high-surface-area current collector and conductor, rGO brings another important benefit. This can be clearly observed when using the Zn microgranules as the electrode. Figure 4c shows the SEM images of the discharged electrodes after 4 cycles. The presence of rGO provides a large area of sites for renucleation and so results in dendrites which are  $<2\ \mu\text{m}$  as opposed to  $\sim 10\ \mu\text{m}$  without the rGO. This leads to additional benefits. The specific capacity was observed to increase by  $\sim 50\%$ , and it was possible to get over 30 cycles from the same electrode with very little loss in capacity (Figure 5).

The addition of rGO to the zinc nanoparticles also prevented their agglomeration and provided a large surface area for the renucleation of ZnO upon discharging, which results in a larger number of particles of smaller size ( $<1\ \mu\text{m}$ ), even after 10 cycles (Figure 5(a)). Having a large surface area template seems to be an effective way of preventing the formation of dendrites in Zn/Ag batteries.

The rGO enhanced battery shows a capacity of up to  $\sim 100\ \text{mAh/g}$ , improved from  $\sim 65\ \text{mAh/g}$  without rGO (Figure 5b). Note the mass used here for gravimetric capacity is the sum of the total mass of active electrodes, both Zn and  $\text{Ag}_2\text{O}$ . It was observed that there is a rapid decrease in capacity in the second cycle, which quickly recovered back to its starting value by cycle 5. This cell was cyclable up to 35 times at near 100% retention, as compared to 4 cycles obtained from the cells without the rGO. It is worth noting that even after 49 cycles, the ZnO rods forming on the electrodes are still less than  $1\ \mu\text{m}$  in size and not expected to result in dendrite mediated device failure (See Supporting Information).

The cells were tested at various discharge rates. The rGO containing cells were found to not only exhibit a higher capacity, but also better high rate capabilities, ascribed to the constant availability of a continuous conducting network.

Further investigations of the sudden drop in capacity beyond  $\sim 30$  cycles, showed that the loss in capacity is not due to the electrode, but in fact damage to the copper current collector. Upon replacing the current collector and the separator, it was possible to recover the cell capacity. 160 cycles were demonstrated by multiple changes to the current collector,

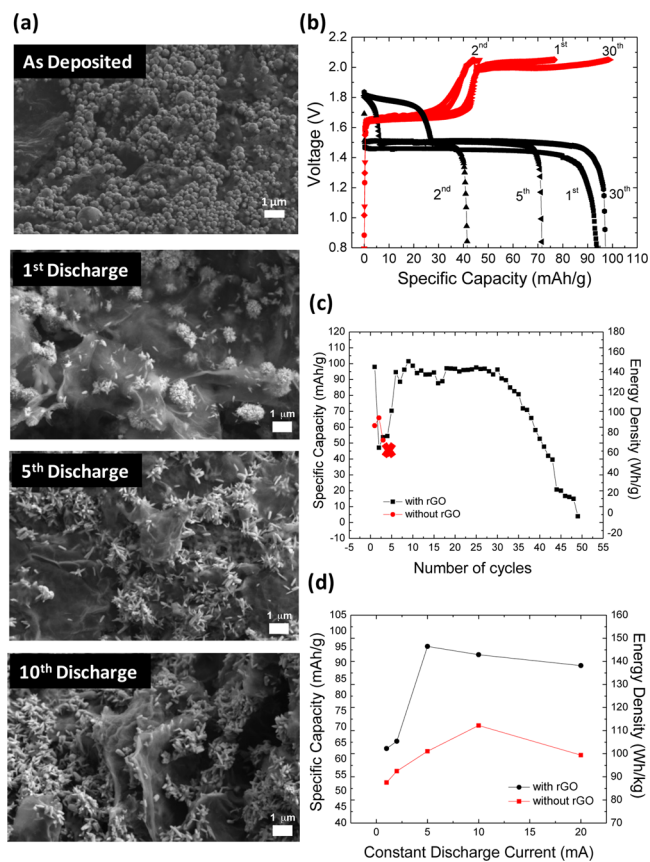


**Figure 5.** (a) SEM images of the Zn/ZnO electrode with the addition of rGO at different stages of the cyclability test. Note the formation of a large number of small particles nucleating on the rGO. (b) Charge/discharge curves of the battery with rGO. (c) Plot of capacity retention with cycling of plain batteries and some with rGO. (d) Comparison of the different discharge rates on battery capacity with and without rGO.

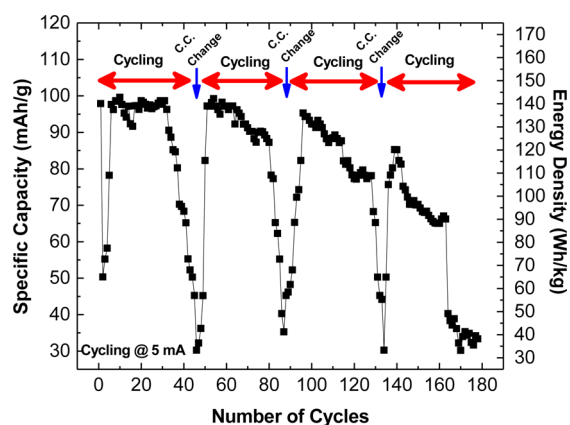


**Figure 6.** Specific capacity of rGO enhanced battery upon cycling. Upon exchange of the copper current collector (c.c.) and the separator, the sudden loss of capacity is recovered and a slow decay from the active electrodes is observed.

showing the suitability of the active electrode material (Figure 6). Further investigation is ongoing for finding more suitable (and stable to corrosion) current collectors.

In summary, we have developed new hybrid electrodes for rechargeable zinc/silver oxide batteries with enhanced electrochemical properties compared to the standard counterpart. In particular, rGO was tested as the conductive additive in the



zinc/silver oxide cells using nanosized and micrometer-sized active electrode materials.

The results demonstrate that an rGO network improves the conductivity of electrodes resulting in enhanced capacity, cycling performance, and rate capabilities of the composite.

## EXPERIMENTAL SECTION

**Electrode Preparation.** The anode paste was produced by blending of as-received Zinc nanopowder (Sigma-Aldrich, <50 nm,  $\geq 99\%$  basis) and rGO (Abalonyx AS, Batch no: RS-0052) in a ratio of 20:1 (Zn/rGO) with 5% of PTFE (60 wt % dispersion in H<sub>2</sub>O, Sigma) as binder. Graphene oxide (GO) prepared by Abalonyx, Norway, according to a modified Hummers method.<sup>30,31</sup> Semidry GO with about 10% humidity was subsequently flashed at 200 °C to produce reduced graphene oxide (rGO). A 100  $\mu\text{m}$  thick Zn foil (Advent Research Materials, 99.99%) of area 1  $\text{cm}^2$  as well as large ( $\sim 100 \mu\text{m}$ ) Zn particles (Aldrich, purum >99%) were also tested as reference anode materials. The cathode was a mixture of silver oxide powder (Sigma-Aldrich, Ag<sub>2</sub>O,  $\geq 99.0\%$ ,  $\sim \text{few } \mu\text{m}$ ) and rGO with 5% PTFE in the same ratio with that of the anode. Monovalent silver oxide is used as it is much more stable than divalent in alkaline solution and has only one step flat discharge curve, despite a lower theoretical capacity vs divalent AgO. The resulting cathode and anode were thoroughly mixed in ambient conditions to achieve homogeneous mixtures and then the resulting paste was spread over a 1  $\text{cm}^2$  area graphite plate.

Typical zinc/silver oxide batteries use aqueous solutions of potassium hydroxide (KOH) or sodium hydroxide (NaOH) as the ionic conductive electrolyte. KOH was used in this work, because of its higher conductivity, allowing the discharge of battery over a wider range of currents. Different concentrations of potassium hydroxide (KOH) aqueous solution were prepared. Zinc oxide nanopowder (Sigma-Aldrich, <100 nm) was dissolved in KOH to supply zincate ions to the medium to reduce the solubility of the zinc electrode.<sup>10</sup>

The cells are assembled by sandwiching an electrolyte soaked cellulose separator between two pieces of as deposited and dried electrodes. Double-sided copper tape was used as current collector and glass slides placed externally for rigidity. The whole structure was sealed to prevent drying of the electrolyte.

**Electrochemical Characterization.** Cell cycling was conducted using a purpose built setup running on a computer controlled Keithley 2400 source meter. All cells were repeated multiple times to check for consistency. Cycling was done in constant current mode. Electrode morphology was characterized with a field emission scanning electron microscope (Carl Zeiss Sigma VP) by disassembling and drying discharged cells prior to imaging. Disassembled electrodes were not reutilized.

## ASSOCIATED CONTENT

### Supporting Information

Further characterization and optimization data of the electrodes used in this work. Surface area characterization and energy density data is included. Data on the optimization of the battery composition are also shown, including the optimization of rGO/active material ratio, the amount of Zn used in the anode, and the concentration of KOH in the electrolyte. The morphology of zinc nanoparticles/rGO composite after 50 cycles is also shown. This material is available free of charge via the Internet at <http://pubs.acs.org>.

## AUTHOR INFORMATION

### Corresponding Author

\*E-mail: [pv237@cam.ac.uk](mailto:pv237@cam.ac.uk)

### Notes

The authors declare no competing financial interest.

## ACKNOWLEDGMENTS

The authors acknowledge Rune Wendelbo from Abalonyx for providing rGO samples and Dr. Tim Butler for his help with battery testing software.

## REFERENCES

- (1) Cheng, F. Y.; Chen, J.; Gou, X. L.; Shen, P. W. High-Power Alkaline Zn–MnO<sub>2</sub> Batteries Using  $\gamma$ -MnO<sub>2</sub> Nanowires/Nanotubes and Electrolytic Zinc Powder. *Adv. Mater.* **2005**, *17*, 2753–2756.
- (2) Yang, C. C.; Lin, S.-J. Improvement of High-Rate Capability of Alkaline Zn–MnO<sub>2</sub> Battery. *J. Power Sources* **2002**, *112*, 174–183.
- (3) Hiralal, P.; Imaizumi, S.; Unalan, H. E.; Matsumoto, H.; Minagawa, M.; Rouvala, M.; Tanioka, A.; Amaratunga, G. A. J. Nanomaterial-Enhanced All-Solid Flexible Zinc-Carbon Batteries. *ACS Nano* **2010**, *4*, 2730–2734.
- (4) Smith, D. F.; Graybill, G. R.; Grubbs, R. K.; Gucinski, A. J. New Developments in Very High Rate Silver Oxide Electrodes. *J. Power Sources* **1997**, *65*, 47–52.
- (5) Karpinski, A. P.; Makovetski, B.; Russell, S. J.; Serenyi, J. R.; Williams, D. C. Silver–Zinc: Status of Technology and Applications. *J. Power Sources* **1999**, *80*, 53–60.
- (6) Philips, J.; Mohanta, S.; Geng, M.; Barton, J.; McKinney, B.; Wu, J. Environmentally Friendly Nickel-Zinc Battery for High Rate Application with Higher Specific Energy. *ECS Trans* **2009**, *16*, 11–17.
- (7) Gupta, N.; Toh, T.; Fatt, M. W.; Mhaisalkar, S.; Srinivasan, M. Paper Like Free-Standing Hybrid Single-Walled Carbon Nanotubes Air Electrodes for Zinc–Air Batteries. *J. Solid State Electrochem.* **2012**, *16*, 1585–1593.
- (8) Lee, D. U.; Park, H. W.; Higgings, D.; Nazar, L.; Chen, Z. Highly Active Graphene Nanosheets Prepared via Extremely Rapid Heating as Efficient Zinc-Air Battery Electrode Material. *J. Electrochem. Soc.* **2013**, *160*, F910–F915.
- (9) McLarnon, F. R.; Cairns, E. J. The Secondary Alkaline Zinc Electrode. *J. Electrochem. Soc.* **1991**, *138*, 645–664.
- (10) Karpinski, A. P.; Schiffer, S. F.; Karpinski, P. A. *Handbook of Batteries*. Linden, D., Reddy, T. B., Eds.; McGraw-Hill: New York, 2011; Chapter 33, pp 981–1010.
- (11) Skelton, J.; Serenyi, R. Improved Silver/Zinc Secondary Cells for Underwater Applications. *J. Power Sources* **1997**, *65*, 39–45.
- (12) Scrosati, B.; Hassounab, J.; Sun, Y.-K. Lithium-Ion Batteries. A Look into the Future. *Energy Environ. Sci.* **2011**, *4*, 3287–3295.
- (13) Ullah, S.; Badshah, A.; Ahmed, F.; Raza, R.; Altaf, A. A.; Hussain, R. Electrodeposited Zinc Electrodes for High Current Zn/AgO Bipolar Batteries. *Int. J. Electrochem. Sci.* **2011**, *6*, 3801–3811.
- (14) Aktas, S. Silver Recovery from Spent Silver Oxide Button Cell. *Hydrometallurgy* **2010**, *104*, 106–111.
- (15) Gaines, L. Secondary Silver-Zinc Battery Technology. *J. Electrochem. Soc.: Rev. and News* **1969**, 61C–67C.
- (16) Bass, K.; Mitchell, P. J.; Wilcox, G. D. Methods for the Reduction of Shape Change and Dendritic Growth in Zinc-Based Secondary Cells. *J. Power Sources* **1991**, *35*, 333–351.
- (17) Ullah, S.; Ahmed, F.; Badshah, A.; Altaf, A. A.; Raza, R.; Lal, B.; Hussain, R. Solvothermal Preparation of ZnO Nanorods as Anode Material for Improved Cycle Life Zn/AgO Batteries. *PLoS One* **2013**, *8*, e75999.
- (18) Shivkumar, R.; Kalaignan, G. P.; Vasudevan, T. Effect of Additives on Zinc Electrodes in Alkaline Battery Systems. *J. Power Sources* **1995**, *55*, 53–62.
- (19) Braam, K. T.; Volkman, S. K.; Subramanian, V. Characterization and Optimization of a Printed, Primary Silver–Zinc Battery. *J. Power Sources* **2012**, *199*, 367–372.
- (20) Ho, C. C.; Murata, K.; Steingart, D. A.; Evans, J. W.; Wright, P. K. A Super Ink Jet Printed Zinc–Silver 3D Microbattery. *J. Micromech. Microeng.* **2009**, *19*, 094013.
- (21) Yan, C.; Wang, X.; Cui, M.; Wang, J.; Kang, W.; Foo, C. Y.; Lee, P. S. Stretchable Silver-Zinc Batteries Based on Embedded Nanowire Elastic Conductors. *Adv. Energy Mater.* **2014**, *4*, 1301396.

(22) Qui, B.; Zhao, X.; Xia, D. In Situ Synthesis of CoS<sub>2</sub>/RGO Nanocomposites with Enhanced Electrode Performance for Lithium-Ion Batteries. *J. Alloys Compd.* **2013**, *579*, 372–376.

(23) Guzman, R. C.; Yang, J.; Cheng, M. M.-C.; Salley, S. O.; Ng, K. Y. S. A Silicon Nanoparticle/Reduced Graphene Oxide Composite Anode with Excellent Nanoparticle Dispersion to Improve Lithium Ion Battery Performance. *J. Mater. Sci.* **2013**, *48*, 4823–4833.

(24) Zhu, X.; Wu, W.; Liu, Z.; Li, L.; Hu, J.; Dai, H.; Ding, L.; Zhou, K.; Wang, C.; Song, X. A Reduced Graphene Oxide-Nanoporous Magnetic Oxide Iron Hybrid as an Improved Anode Material for Lithium Ion Batteries. *Electrochim. Acta* **2013**, *95*, 24–28.

(25) Sun, Y.; Yang, S.-B.; Lv, L.-P.; Lieberwirth, I.; Zhang, L.-C.; Ding, C.-X.; Chen, C.-H. A Composite Film of Reduced Graphene Oxide Modified Vanadium Oxide Nanoribbons as a Free Standing Cathode Material for Rechargeable Lithium Batteries. *J. Power Sources* **2013**, *241*, 168–172.

(26) Yan, M.; Wang, F.; Han, C.; Ma, X.; Xu, X.; An, Q.; Xu, L.; Niu, C.; Zhao, Y.; Tian, X.; Hu, P.; Wu, H.; Mai, L. Nanowire Templated Semihollow Bicontinuous Graphene Scrolls: Designed Construction, Mechanism, and Enhanced Energy Storage Performance. *J. Am. Chem. Soc.* **2013**, *135*, 18176–18182.

(27) Xu, J.-J.; Wang, Z.-L.; Xu, D.; Zhang, L.-L.; Zhang, X.-B. Tailoring Deposition and Morphology of Discharge Products Towards High-Rate and Long-Life Lithium-Oxygen Batteries. *Nat. Commun.* **2013**, *4*, 2438.

(28) Malik, R.; Burch, D.; Bazant, M.; Ceder, G. Particle Size Dependence of the Ionic Diffusivity. *NanoLett.* **2010**, *10*, 4123–4127.

(29) Wagemaker, M.; Borghols, W. J. H.; Mulder, F. M. Large Impact of Particle Size on Insertion Reactions. A Case for Anatase Li<sub>x</sub>TiO<sub>2</sub>. *J. Am. Chem. Soc.* **2007**, *129*, 4323–4327.

(30) Wendelbo, R. Fotedar, S. Grafénderivatpasta, Norw. Patent 20120917, August 16, 2012.

(31) Hummers, W. S.; Offeman, R. E. Preparation of graphitic oxide. *J. Am. Chem. Soc.* **1958**, *80*, 1339–1339.